Sensitivity of nucleon-nucleus scattering to the off-shell behavior of on-shell equivalent *NN* potentials

H. F. Arellano,[1] F. A. Brieva,[1] M. Sander,[2] and H. V. von Geramb[2]
[1]*Departamento de Física, Facultad de Ciencias Físicas y Matemáticas, Universidad de Chile, Casilla 487-3, Santiago, Chile*
[2]*Theoretische Kernphysik, Universität Hamburg, Luruper Chaussee 149, D-22761, Hamburg, Germany*
(Received 16 April 1996)

The sensitivity of nucleon-nucleus elastic scattering to the off-shell behavior of realistic nucleon-nucleon interactions is investigated when on-shell equivalent nucleon-nucleon potentials are used. The study is based on applications of the full-folding optical model potential for an explicit treatment of the off-shell behavior of the nucleon-nucleon effective interaction. Applications were made at beam energies between 40 and 500 MeV for proton scattering from ^{40}Ca and ^{208}Pb. We use the momentum-dependent Paris potential and its local on-shell equivalent as obtained with the Gelfand-Levitan and Marchenko inversion formalism for the two nucleon Schrödinger equation. Full-folding calculations for nucleon-nucleus scattering show moderate fluctuations in the corresponding observables. This sets narrow margins within which off-shell features of the nucleon-nucleon interaction can be resolved. Based on these results, inversion potentials were also constructed directly from phenomenological phase shifts (SM94). Their use in nucleon-nucleus scattering at intermediate energies provides an improved description of the data relative to those obtained from current realistic potential models. [S0556-2813(96)04110-6]

PACS number(s): 24.10.Ht, 13.75.Cs, 21.30.Fe, 25.40.Cm

I. INTRODUCTION

Theoretical studies of the two-nucleon interactions in their off-shell domain have a long-standing tradition [1] and this topic is of renewed interest for designated experiments at several accelerators laboratories. Few- and many-body systems offer the possibility for such studies but not seldom have such endeavors ended prematurely due to lack of statistics in data taking or an incomplete and inconclusive theory. Current interest in this issue comes from theory groups who have independently developed *NN* potentials which account reasonably well for two-body phase shifts at energies below the pion production threshold [2–4]. These potentials are manifestly different in their off-shell behavior. A means of measurable discrimination among them would be very valuable for a comprehensive understanding of their particular features.

In the past much hope was given to *NN* bremsstrahlung as this three body reaction is, within a Born approximation, theoretically well defined [5,6]. This simple reaction mechanism provides an explicit connection between the $(NN\gamma)$ observables and half-off-shell *NN* *t* matrices. Using the available theoretical developments in the field it is now possible to explain the available data with different *NN* potentials provided they agree with the *NN* data very well. This result has been independently validated and remains a surprise in view of the obvious differences in the half-off-shell *t* matrices from different potential models. In other words, the expectation that on-shell equivalent potentials would provide distinctive bremsstrahlung predictions was disillusioned with more complete and reliable calculations.

It can be argued that bremsstrahlung involves only half-off-shell *t* matrices and thus this reaction is rather confined in phase space. Microscopic models of nucleon-nucleus (NA) scattering in the full-folding model [7,8] do not suffer from such limitations as the optical potential depends explicitly upon the effective interaction fully off shell. Thus, this constitutes an alternative framework for investigating the *NN* interaction off shell.

Recently, significant advances have been made in accurately handling the off-shell degrees of freedom in *NA* elastic scattering [7–12]. Here, studies have demonstrated that an accurate treatment of the off-shell behavior of the *NN* interaction is needed for a proper account of the theory. Irrespective of obvious improvements in describing the data at projectile energies below 400 MeV, the calculations still show some systematic deficiencies. In particular the misfit of spin observables at momentum transfers below $\sim 1\ \mathrm{fm}^{-1}$ is not understood. The origin of such discrepancies with the data could be attributed to phenomenological limitations of the bare *NN* potential, particularly at the higher energies, to the simplifications in the model for the *NN* effective interaction, or to the fact that the optical model potential has only been developed to its lowest order. Above 400 MeV, results from the full-folding model deteriorate quickly [7]. At these energies, however, the underlying *NN* potentials are being applied beyond their domain of design and therefore an assessment of the theory needs a more adequate description of the bare two-body interaction.

Despite the significant advances in full-folding model calculations it remains difficult to identify, at the level of the scattering observables, distinctive off-shell features of *NN* interactions. This difficulty is mainly attributed to non-negligible differences on shell among the available realistic *NN* potentials [13].

In this paper we investigate the sensitivity of *NA* scattering when using *NN* potentials which are equivalent on shell. For that purpose we have chosen the Paris potential in its full momentum-dependent form and its local equivalent potential generated with the Gelfand-Levitan-Marchenko inversion

formalism. The inversion potential exhibits different off-shell continuations as does the original Paris potential. These differences and associated correlations are investigated in the full-folding *NA* optical model.

We find for these two alternative potentials overall differences of about 10% in their corresponding *NA* scattering observables. Since the theory of the optical potential is still not satisfactory within this level of precision, it becomes infeasible to use this framework to infer information about features off shell of the *NN* interaction. More generally, however, this result provides a practical means to connect *NN* and *NA* scattering. As a mediating formalism Gelfand-Levitan-Marchenko quantum inversion may use only experimental *NN* data as input and thus link model-independent two-body with many-body data.

This article is organized as follows. In Sec. II we outline the theoretical background for the present work. We introduce and discuss aspects and assumptions implicit in the Gelfand-Levitan and Marchenko inversion methods as well as the *in-medium* full-folding model of the optical potential for *NA* elastic scattering. In Sec. III we discuss the sensitivity of *NA* scattering to off-shell features of the *NN* interaction by calculating scattering observables from the Paris potential and from an inversion potential constructed from the same Paris phase shifts (Paris inversion). In this way the analysis becomes focused on intrinsic differences between the two potentials off-shell. In Sec. IV we construct inversion *NN* potentials directly from the *NN* data, including approximately the *NN* phase shifts above pion production threshold as a way to guide the intermediate energy properties of the potential. Calculations for proton-nucleus elastic scattering in the 40–500 MeV range and from different targets are also discussed. Finally, in Sec. V we present a summary and draw conclusions from this work.

II. THEORETICAL BACKGROUND

A. Two nucleon potentials from quantum inversion

In the last few years, boson exchange models have provided a practical framework to construct reasonably accurate realistic *NN* potentials. Representative among these are the Nijmegen [14] and Bonn potentials [3]. The Paris potential also belongs to this category and describes the long- and medium-range interactions with single- and correlated two-pion exchange and heavier meson exchanges [2]. It fits the experimental two nucleon data reasonably well and has extensively been applied to calculations of microscopic optical model potentials for *NA* scattering at low and medium energies. This potential is generally used in its Yukawa parametrization including an explicit momentum-dependent term [2]

$$V=V_a+\frac{\hbar^2}{m}p^2V_b+V_b\frac{\hbar^2}{m}p^2, \tag{1}$$

where m is the nucleon mass and p the relative momentum operator. This momentum dependence emulates a hard core repulsion and produces a divergence of the phase shift $\delta(k)$ as $k\rightarrow\infty$. When compared with the data, the Paris potential fits quite well the phase shift at energies up to 280 MeV. Above this energy we notice a rapidly increasing divergence. This characteristic strong repulsion at short distances is easy to identify in cross section and spin observables of *NA* scattering and reactions [15]. Despite this weakness we have chosen the Paris potential because of its simplicity and our confidence in the numerics of our Lippmann-Schwinger and Bethe-Goldstone calculations with it.

In this work we aim to disclose effects which are caused by the momentum dependence and high energy phase shift discrepancies of the genuine Paris potential in off-shell t and g matrices. To this purpose we use the recently developed Gelfand-Levitan-Marchenko inversion of partial wave radial Schrödinger equations to generate a local potential phase equivalent to the Paris potential. These inversion algorithms distinguish inversion for single and coupled channels, with and without a Coulomb reference potential [16]. In other words, we obtain separately the hadronic part of the *NN* interaction from any set of *np* and *pp* phase shifts.

The strong interaction inversion potentials $V(r;LSJ,T;np)$ and $V(r;LSJ,T;pp)$ are numerical solutions of Gelfand-Levitan or Marchenko integral equations

$$K(r,r')+F(r,r')+\int K(r,s)F(s,r')ds=0 \tag{2}$$

and

$$V(r)=\pm\frac{d}{dr}K(r,r) \tag{3}$$

for any specified radius and they are determined channel by channel. The input kernel $F(x,y)$ is computed with the spectral information, Jost functions, or S matrices including deuteron binding energy and normalization constants. We use quantum inversion as transformation of given real phase shifts which are specified within a finite energy interval

$$\delta(k)\sim\delta(E)=\{\delta(k)|E=[0,E_{\max}]|k=[0,k_{\max}]\}. \tag{4}$$

Thereafter they are smoothly extrapolated with a rational function which decays asymptotically [17],

$$\delta(E)\sim\delta(k)=\{\delta(k)|k\geqslant k_{\max}|\lim_{k\rightarrow\infty}\delta(k)\sim k^{-1}\}. \tag{5}$$

This transformation is unique for the class of potentials we are interested in and which we assume physically significant. The resulting inversion potentials are real and local.

It is evident that this inversion procedure produces a restricted phase-equivalent potential to the Paris potential. The limited data input $\delta(E)$ for $0\leqslant E\leqslant E_{\max}$ is used to control the range of equivalence and the extrapolation thereafter to control the softness of the short range core interaction.

B. In-medium full-folding optical potential

The optical potential for *NA* elastic scattering can be casted as the convolution of an antisymmetrized effective interaction with the target ground-state single-particle wave functions [18–21,9]. In momentum space this one-body operator reads

$$U(\vec{k}',\vec{k};E)=\int d\vec{p}\,d\vec{p}'\sum_{\alpha\leqslant\epsilon_F}\phi_\alpha^\dagger(\vec{p}')\times\langle\vec{k}',\vec{p}'|F(E+\epsilon_\alpha)|\vec{k},\vec{p}\rangle_A\phi_\alpha(\vec{p}),\qquad(6)$$

where E represents the energy of the incoming projectile and $\{\phi_\alpha,\epsilon_\alpha\}$ are the target ground-state single-particle wave functions and corresponding energies. The momenta $\vec{k}(\vec{k}')$ and $\vec{p}(\vec{p}')$ correspond to the initial (final) momenta of the projectile and target struck nucleon, respectively. The two-nucleon interaction in Eq. (6) accounts for multiple scattering of nucleons to all orders in the ladder approximation [18,22]. Although a general expression for this matrix can formally be defined, its practical implementation requires the device of a dynamical model for the effective two-nucleon interaction in the nucleus. The procedure we follow is that introduced in Ref. [9], where translational invariance of the two-nucleon scattering in free space or infinite nuclear matter suggests the following ansatz for the two-body matrix:

$$\langle\vec{k}',\vec{p}'|F(\omega)|\vec{k},\vec{p}\rangle=\frac{1}{(2\pi)^3}\int d\vec{R}e^{i\vec{R}\cdot(\vec{Q}-\vec{Q}')}\times\langle\vec{\kappa}'|f_{(\vec{Q}+\vec{Q}')/2}(\omega;\vec{R})|\vec{\kappa}\rangle.\qquad(7)$$

Here we have defined the initial and final two-nucleon center-of-mass (c.m.) momenta

$$\vec{Q}=\vec{k}+\vec{p},\quad \vec{Q}'=\vec{k}'+\vec{p}',\qquad(8)$$

and the corresponding relative momenta by

$$\vec{\kappa}=\tfrac{1}{2}(\vec{k}-\vec{p}),\quad \vec{\kappa}'=\tfrac{1}{2}(\vec{k}'-\vec{p}').\qquad(9)$$

The function $\langle\vec{\kappa}'|f_{\vec{Q}}(\omega;\vec{R})|\vec{\kappa}\rangle$ corresponds to the matrix elements of a reduced two-body effective interaction. In the case of no dependence of the f matrix upon the spatial coordinate $(\vec{R})$ one restores total momentum conservation of the interacting pair as the radial integral in Eq. (7) leads to a c.m.-momentum-conserving Dirac δ function.

A calculable expression for the optical potential *in medium* emerges after a systematic reduction of the many-body propagator when represented in terms of the target ground-state spectral function [9]. To lowest order in a series expansion of the two-body propagator in a finite nucleus, this interaction can be identified with the g-matrix solution of the Brueckner-Bethe-Goldstone equation for interacting nucleons in infinite nuclear matter and evaluated at nuclear density $\rho(R)$ in the nucleus. Furthermore, it becomes convenient to substitute the single particle energies ϵ_α by an average value and to use the Slater or Campi-Bouyssy approximations [23,24] to represent the ground-state mixed density, i.e.,

$$\rho(\vec{p}',\vec{p})=\sum_{\alpha\leqslant\epsilon_F}\phi_\alpha^\dagger(\vec{p}')\phi_\alpha(\vec{p})\approx\frac{4}{(2\pi)^3}\int d\vec{R}e^{i(\vec{p}'-\vec{p})\cdot\vec{R}}\rho(R)\times\left\{\frac{1}{\hat{\rho}(R)}\int d\vec{P}\Theta[\hat{k}(R)-P]\right\},\qquad(10)$$

where $\rho(R)$ is the local nuclear density at coordinate $\vec{R}$ and $\vec{P}$ represents the struck nucleon mean momentum defined by

$$\vec{P}=\tfrac{1}{2}(\vec{p}+\vec{p}').\qquad(11)$$

The local momentum function $\hat{k}(R)$ sets the range of variation of the struck nucleon mean momenta upon collisions with the projectile and is obtained from the Slater or Campi-Bouyssy [23] prescriptions. The local density function $\hat{\rho}(R)$ is defined in terms of the local momentum function by

$$\hat{\rho}(R)=\frac{2}{3\pi^2}\hat{k}^3(R).\qquad(12)$$

With the above the optical potential can be expressed in terms of the nuclear density and a Fermi-averaged effective interaction obtained from interacting nuclear matter. This interaction retains nuclear medium correlations associated with the nuclear mean fields and Pauli blocking. The *in-medium* full-folding optical potential then reads

$$U(\vec{k}',\vec{k};E)=\frac{4}{(2\pi)^3}\int d\vec{R}e^{i\vec{q}\cdot\vec{R}}\rho(R)\frac{1}{\hat{\rho}(R)}\int d\vec{P}\Theta[\hat{k}(R)-P]\times\langle\tfrac{1}{2}(\vec{K}-\vec{P}-\vec{q})|g_{\vec{K}+\vec{P}}(E+\overline{\epsilon;\vec{R}})|\tfrac{1}{2}(\vec{K}-\vec{P}+\vec{q})\rangle_A,\qquad(13)$$

with the definitions

$$\vec{K}=\tfrac{1}{2}(\vec{k}+\vec{k}'),\quad \vec{q}=\vec{k}-\vec{k}'.\qquad(14)$$

Thus, the optical potential requires the calculation of g matrices off shell as their relative momenta obey no constraints apart from those imposed by the ground-state mixed density of the target. Furthermore, no assumptions are introduced on the nature of the momentum dependence of the optical potential, thus retaining all nonlocalities arising from the genuine momentum dependence of the NN effective interaction. Actual calculations involve determining g matrices at several densities and over a wide range of total c.m. momenta, features fully accounted for in the present work.

In the context of a medium-independent internucleon interaction, as when the free t matrix is used to represent the NN effective interaction, the integral over the spatial coordinate in Eq. (13) can be performed separately from the motion of the target nucleons. With the use of Eq. (10) for the mixed density one recovers the expression for the full-folding optical potential in the zero density approximation [7], namely, $U(\vec{k}',\vec{k};E)\rightarrow U_0(\vec{k}',\vec{k};E)$, where

$$U_0(\vec{k}',\vec{k};E)=\int d\vec{P}\rho(\vec{P}+\tfrac{1}{2}\vec{q},\vec{P}-\tfrac{1}{2}\vec{q}) \times\langle\tfrac{1}{2}(\vec{K}-\vec{P}-\vec{q})|t_{\vec{K}+\vec{P}}(E+\overline{\epsilon})|\tfrac{1}{2}(\vec{K}-\vec{P}+\vec{q})\rangle_A . \quad (15)$$

The dependence of the optical potential on off-shell t matrices becomes explicit in the above expression. The feasibility of the full-folding model to investigate particular signatures of the effective interaction off shell will depend on the sensitivity of NA scattering observables to the use of t matrices with manifestly distinctive behaviors off shell. An important constraint for such a study is that the effective interactions, t matrices in this limit, agree on shell. To the extent this constraint is met one can attain the differences in the NA scattering observables to the differences of the interactions off shell.

A simple kinematical effect usually overlooked, but explicitly accounted for in our calculations, is that the full-folding approach calls for matrix elements of energy $E+\overline{\epsilon}$ in the laboratory frame. In the limit of the free t matrix for the NN interactions, the energy of the interacting pair in its c.m. is given by $E+\overline{\epsilon}-(1/4m)(\vec{K}+\vec{P})^2$. Therefore, the maximum energy of the pair in its c.m. is $E+\overline{\epsilon}$, the energy of the beam plus the average binding energy of the target nucleons. In the case of optical potentials for nucleons at 500 MeV, for instance, t matrices of up to ~ 1 GeV in the laboratory frame are required. This more demanding sampling of the NN effective interaction is a result of the unconstrained kinematics allowed by the Fermi motion of the nucleons in the nucleus.

A few comments are pertinent regarding further approximations in the treatment of the t matrix and which limit an assessment of the off-shell behavior of the NN interaction in NA scattering. A simplifying assumption, commonly used in alternative full-folding calculations [10,11], is that the t matrix varies very weakly with respect to the NN c.m. momentum $\vec{K}+\vec{P}$. Thus, the magnitude of this momentum is fixed to the (asymptotic) on-shell value of the incoming projectile, K_0, and the t matrix is approximated by

$$t_{\vec{K}+\vec{P}}(\omega)\approx t_{\vec{K}_0}(\omega). \quad (16)$$

Thus, t matrices are evaluated at a fixed energy equal, in the NN c.m., to one-half the energy of the beam. Here one has neglected all effects associated with the Fermi motion in the NN c.m. momentum dependence. The resulting full-folding calculations sample the t matrix off shell through the dependence on $\vec{P}$ in the relative momenta exclusively [see Eq. (15)]. This approximation seems adequate at beam energies near 300 MeV. Its application at lower or higher energies, however, needs further considerations as the NN t matrix exhibits a sizable NN c.m. momentum dependence [8]. In the low energy region, apart from the fact that medium effects need to be incorporated in the model, the underlying kinematics prescribed by the full-folding leads to the sampling of the t matrix in regions where it varies significantly as the low energy behavior of the interactions becomes dominant. In the high energy regime, in turn, difficulties arise from the opening of inelastic channels such as those associated with pion production or Δ resonances. The actual merit of the theory of the optical potential needs to be assessed with a consistent incorporation of such additional degrees of freedom.

C. *NN* effective interaction

In the present approach, correlations associated with interacting nucleons in the nuclear medium are obtained from the NN effective interaction defined by the Brueckner-Bethe-Goldstone equation for symmetric nuclear matter. In momentum representation, the g matrix for interacting nucleons of total c.m. momentum $\vec{Q}$, starting energy ω, and nuclear density ρ satisfies

$$\langle\vec{\kappa}'|g_{\vec{Q}}(\omega;\vec{R})|\vec{\kappa}\rangle=\langle\vec{\kappa}'|V|\vec{\kappa}\rangle + \int d\vec{\kappa}''\langle\vec{\kappa}'|V|\vec{\kappa}''\rangle\lambda^{\rm NM}_{\vec{Q}}(\vec{\kappa}'';\omega;k_F) \times\langle\vec{\kappa}''|g_{\vec{Q}}(\omega;\vec{R})|\vec{\kappa}\rangle, \quad (17)$$

with k_F the nuclear matter Fermi momentum determined from the nuclear density *via*

$$k_F=\left(\frac{3\pi^2}{2}\rho(R)\right)^{1/3}. \quad (18)$$

The two-body propagator $\lambda^{\rm NM}$ models both Pauli blocking and the nuclear mean-field effects in the propagation of intermediate states,

$$\lambda^{\rm NM}_{\vec{Q}}(\vec{q};\omega;k_F)=\frac{\mathcal{Q}(P_+;P_-;k_F)}{\omega+i\eta-\epsilon(P_+;k_F)-\epsilon(P_-;k_F)}, \quad (19)$$

with $P_\pm=|\frac{1}{2}\vec{Q}\pm\vec{q}|$ and $\mathcal{Q}$ the Pauli blocking function

$$\mathcal{Q}(P_+;P_-;k_F)=\Theta[\epsilon(P_+;k_F)-\epsilon_F]\Theta[\epsilon(P_-;k_F)-\epsilon_F]. \quad (20)$$

Here the single-particle energies ϵ are defined in terms of the self-consistent nuclear matter fields, $U_{\rm NM}$,

$$\epsilon(k_\alpha;k_F)=\frac{k_\alpha^2}{2m}+{\rm Re}[U_{\rm NM}(k_\alpha;k_F)], \quad (21)$$

where the mean fields $U_{\rm NM}(k;k_F)$ are calculated self-consistently for the underlying bare NN interaction from

$$U_{\rm NM}(k;k_F) =\sum_{\alpha\leqslant\epsilon_F}\langle\tfrac{1}{2}(\vec{k}-\vec{k}_\alpha)|g_{[\vec{k}+\vec{k}_\alpha]}[\epsilon(k)+\epsilon(k_\alpha)]|\tfrac{1}{2}(\vec{k}-\vec{k}_\alpha)\rangle. \quad (22)$$

Actual calculations of these mean fields have been made using the continuous prescription at the Fermi energy [25] and simplifying the Pauli blocking function $\mathcal{Q}$ by its angle-averaged form.

III. PARIS VERSUS PARIS INVERSION

We have used the Paris potential to generate a set of NN phase shifts which are taken as input to calculate the corresponding inversion potential. Thus, we make sure that

Paris and the inversion potential are on-shell equivalent within the numerical accuracy given by our inversion algorithms. The range of energies where the phase shifts are considered does have an effect on the off-shell behavior of the inversion potential. This is observed when calculating optical potentials and corresponding scattering observables using the free t matrix based on inversion potentials constructed from a common set of phase shifts but defined over different energy ranges. Therefore, to ensure that properties of the inversion potential depend solely on the dynamical equations we have verified that a set of Paris phase shifts in the 0–1.3 GeV energy range is sufficient to construct an inversion potential that can be used up to 500 MeV in effective interaction calculations (Sec. II C). Above 1.3 GeV, the inversion algorithm assumes a smooth decrease of the phase shifts to zero [Eq. (5)]. This extrapolation departs strongly from the Paris potential behavior at short distances.

In Fig. 1 we show the Paris phase shifts (crosses) and the phase shifts obtained from its corresponding inversion potential (solid line) for selected NN channels ($L \leqslant 2$) and in the 0–1.2 GeV energy range. By dint of its construction the inversion potential reproduces the input phase shifts with high accuracy. We have allowed an exception for the $^3D_1$ above 400 MeV to avoid oscillations of this channel potential. To prevent them we have incorporated a regularization algorithm which allows for a small change in the phases within a few degrees at the higher energies. This effect can be seen in Fig. 1. In NN bremsstrahlung calculations at 300 MeV [5], for instance, the effect of this deficiency is negligible in the observables and we have verified the same to be valid here. Altogether, we can say that the calculated inversion potential is phase equivalent to the Paris potential. Their differences in a many-body system should come from the intrinsic properties of the two potentials provided the off-shell sampling is compatible with the energy range of equivalence.

The inversion potential differs on its off-shell content from the original Paris potential as the former is static and local, whereas the latter is momentum dependent. These differences and associated correlations to all orders shall be investigated in the context of the full-folding model of the optical potential for NA scattering and as described in Sec. II B.

A. Off-shell effects in NA scattering

We have calculated both t matrices and g matrices from the Paris and its inversion potentials. The inversion scheme was used for all the NN channels with total orbital angular momentum $L \leqslant 3$. For channels with $L > 3$ the genuine Paris potential is used. The NA optical potential was calculated using the g matrix as an effective interaction since medium effects have been proved to be important even for nucleons with incident energies of 400 MeV [9]. The corresponding g matrices were calculated solving Eq. (17) using standard matrix inversion methods [26]. The $\vec{R}$ dependence in the full-folding integral was obtained by calculating g matrices at different densities as obtained from different values for k_F up to 1.4 fm^{-1}. For an accurate off shell sampling of the NN effective interaction, g matrices were calculated at several values of the total NN c.m. momentum in the 0–7 fm^{-1} interval, with higher density of points in the region where it varies most rapidly as a function of the c.m. momentum. Contributions associated with the deuteron bound state singularity were also included [8]. The ground-state nuclear densities and average binding energies [in Eq. (13)] are the same as in Ref. [9].

Calculations of differential cross sections ($d\sigma/d\Omega$) and analyzing powers (A_y) were made for proton elastic scattering from ^{40}Ca and ^{208}Pb in the 40–400 MeV energy range. Results for the spin rotation function have been omitted in this discussion for brevity as they exhibit similar behavior as those observed in A_y. In Figs. 2 and 3 we present the calculated scattering observables, as a function of the center-of-mass scattering angle ($\Theta_{\text{c.m.}}$) in the 40–MeV application, and as a function of the momentum transfer (q) at 400 MeV. The data for $p + ^{40}$Ca scattering at 40 MeV were taken from Ref. [27,28]. In the case of $p + ^{208}$Pb at 400 MeV the data were taken from Ref. [29]. The solid and dashed curves represent results for the Paris potential and corresponding inversion, respectively. Results at different energies and for different targets show comparable quantitative differences. Similar differences are observed in analogous calculations but using the free t matrix as the NN effective interaction.

Some conclusions can be drawn. The two phase-equivalent potentials give a qualitatively similar description of the scattering observables, regardless their very different intrinsic structure. The differences between the two curves in Figs. 2 and 3 reflect the level of sensitivity to the off-shell behavior associated with each underlying NN effective interaction. Quantitatively, we observe up to a 20% difference in the magnitude of the calculated observables due to differences off shell in the effective interaction, a feature that is maintained in the energy range under study. Discrepancies found in the $^3D_1$ state do not alter this finding. Therefore, we may conclude that the full-folding model cannot unambiguously discriminate the off shell differences among on-shell-equivalent NN potentials.

Our results also suggest that the on-shell content of the NN potential becomes crucial for determining its off shell properties. To this regard, the inversion method provides a unique tool to study the behavior of the inversion potential as a function of the energy range where the on-shell equivalence is established. We have proceeded to take a restricted NN energy range (0–400 MeV instead of 0–1.3 GeV) for the Paris phase shifts to construct its corresponding inversion potential. In this case we obtain a significantly different off shell behavior in the NN interaction, as reflected by the differences in the corresponding NA scattering observables. These differences become more pronounced above 200 MeV nucleon incident energies. In turn, when the Paris phase shifts are taken from the 0–3 GeV energy range to construct the inversion potential we observe no further differences in the NA scattering observables (beam energy below 600 MeV) from those obtained using the 0–1.3 GeV energy range. Then, NN potentials which closely account for the NN phase shift data over a wide energy range are essential for assessing the level of completeness of the optical model for NA scattering.

The relatively weak sensitivity to the off shell effects suggests that NN potentials constructed by means of the inver-

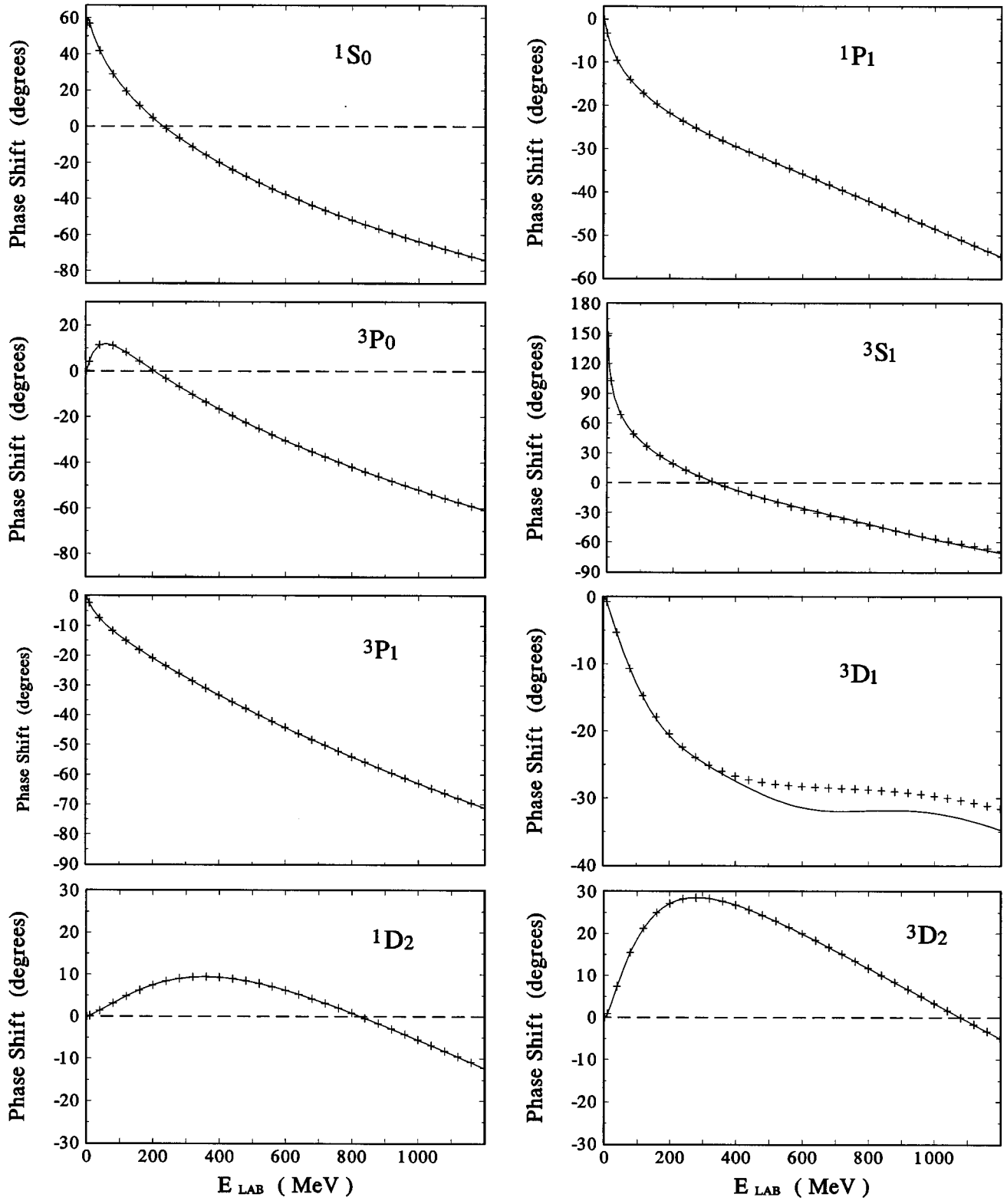

FIG. 1. $L \leqslant 2$ channel phase shifts from the Paris potential (crosses) and from corresponding inversion potential (solid curves).

sion scheme following closely the *NN* data are meaningful and should provide predictions for the full-folding model very close to what would it be obtained from first principles *NN* potentials with a comparable fit to the data.

B. Effective interactions off shell

To illustrate the degree of sensitivity of the *g* matrix upon alternative choices of bare *NN* potentials, we have calculated selected matrix elements relevant for the leading contribution

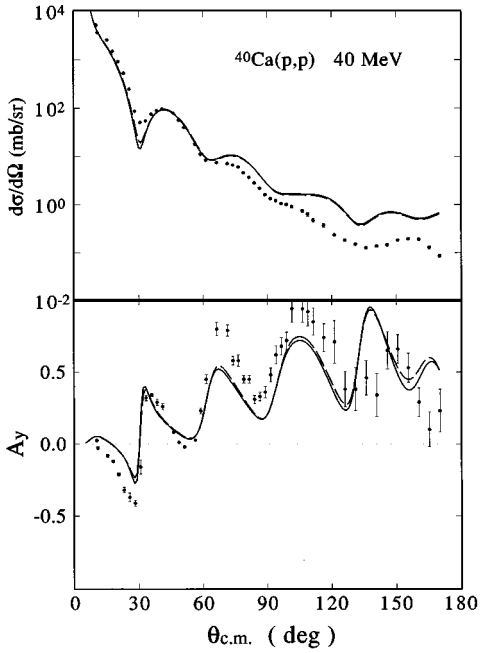

FIG. 2. Scattering observables calculated from the Paris (solid curves) and its corresponding inversion potential (dashed curves) for $p+{}^{40}$Ca at 40 MeV.

to the optical potential. Thus, we consider diagonal g-matrix elements, i.e., $\langle\vec{\kappa}|g_{\vec{Q}_0;k_F}(\omega;\vec{R})|\vec{\kappa}\rangle$, with Q_0 fixed to a single value by $Q_0=\sqrt{2m\omega}$. In the context of the free t matrix ($k_F=0$) this kinematics implies that the on-shell relative momentum occurs for $\kappa=(1/2)Q_0$. Since κ is in general independent of both Q_0 and ω, the resulting function corresponds to off shell elements of the g matrix. For the Paris and its inversion-equivalent potential we have solved Eq. (17) for g in the cases $k_F=0$ fm^{-1} and $k_F=1$ fm^{-1} and for the state $^1S_0$. This is a good example to illustrate the differences at the effective interaction level observed in most of the states. In Fig. 4 we show the corresponding matrix elements, both real and imaginary components, for $\omega=30$, 200, and 400 MeV. The solid and the dashed curves represent results from the Paris potential and its inversion respectively.

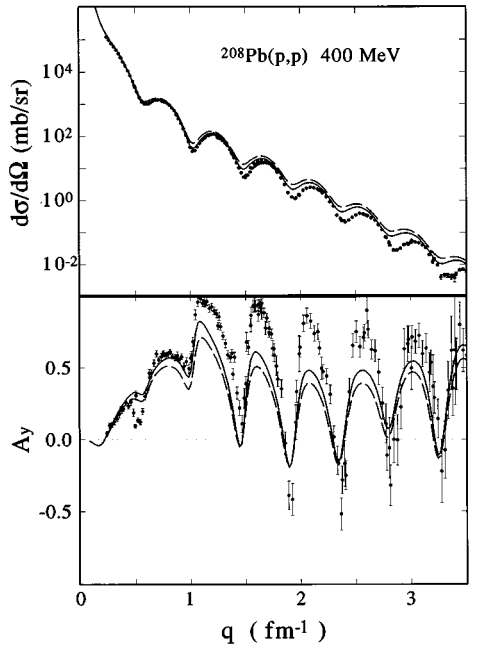

FIG. 3. Scattering observables calculated from the Paris (solid curves) and its corresponding inversion potential (dashed curves) for $p+{}^{208}$Pb at 400 MeV.

Since the Paris potential and its inversion are equivalent on shell, the solid and dashed curves for the t matrix ($k_F=0$) must intercept each other at $\kappa=(1/2)Q_0$ in both their real and imaginary components. This is indeed the case in the figures shown here as the on-shell constraint is explicitly built in the inversion method; this is not necessarily the case, however, for the g matrix as the propagator differs from that in free space by the presence of Pauli blocking and the self-consistent fields. It is interesting to note the different asymptotic behavior ($\kappa\to\infty$) between the Paris and the inversion potentials for both $k_F=0$ and $k_F=1$ fm^{-1}. Whereas all curves tend to zero as κ increases, the one corresponding to the real part of the g matrix for the Paris potential does not. This behavior is consistent with the explicit momentum dependence introduced in the parametrization of the Paris potential, a feature which becomes dominant at high momenta. The extent to which this distinctive behavior is significant in the dynamics of the collision of the projectile with the nucleus needs to be assessed in the context of the elastic scattering observables.

IV. *NA* SCATTERING FROM PHENOMENOLOGICAL *NN* PHASE SHIFTS

In this section we extend the idea of *NN* potentials obtained directly from *NN* phase shifts through the quantum inversion method and its application to *NA* scattering. It is well known that the two-nucleon on-shell amplitudes have changed significantly since the Paris potential parametrization was first published. The importance of using off-shell amplitudes in *NA* scattering is beyond any doubt, but it remains uncertain what details can be resolved. In the previous sections we have shown that two distinct on-shell equivalent potentials—the Paris and its inversion—exhibit similar behaviors near the on-shell value. Thus, with quantum inversion of phase shifts we have a tool to continue the on-shell measurements into the off-shell domain for its use in nucleon-nucleus scattering. For this purpose, we have calculated a *NN* inversion potential based on the SM94 phase-shift analysis of Arndt and collaborators [30]. Thus we intend to show that an accurate description of the *NN* on-shell amplitudes by realistic potentials is required before finer details of the off shell continuation and other reaction aspects should be addressed.

One problem we face is the choice of a meaningful energy range where the phase shifts are to be taken from. Indeed, in order to be consistent with the inversion scheme, a set of real phase shifts are needed. Strictly speaking, this sets a limit for the energy range at pion production threshold ($\sim$300 MeV). However, the study with the Paris potential in Sec. III shows that phase shifts at much higher energies are required by the inversion method. Therefore, a criterion for incorporating them is needed.

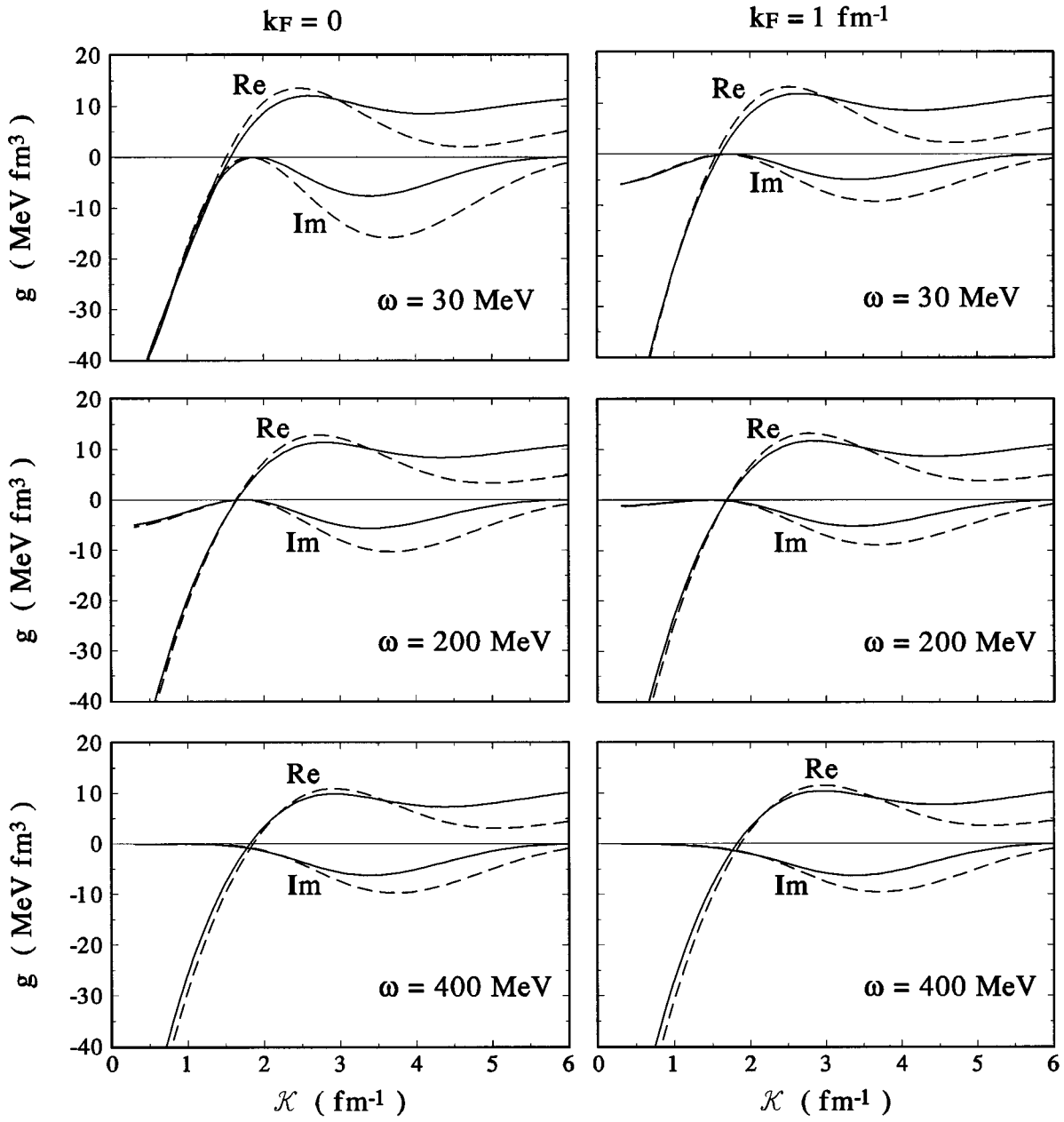

FIG. 4. Behavior of the diagonal elements of the g matrix for the state $^1S_0$ as a function of the relative momentum and for $\omega=30$ MeV (top), $\omega=200$ MeV (center), and $\omega=400$ MeV (bottom). The figures on the left correspond to $k_F=0$ (t matrix) and those on the right to $k_F=1.0$ fm^{-1} The solid curves represent results from the genuine Paris potential. The dashed curves correspond to results obtained from inversion potentials based on the Paris phase shifts.

Our approach is as follows. In order to account approximately for the energy trend that the phase shifts have above the pion production threshold, we have neglected the imaginary component of the phase shifts and retained only their real components. This affects mainly the $^1D_2$ and $^3F_3$ channels, the ones which exhibit the most pronounced absorption [30]. Thus we can construct a real NN inversion potential from a set of real phase shifts. The range of energy considered here for the inversion is 0–1.3 GeV. Irrespective of the limitations implied by these assumptions, we believe that the use of such NN potentials shall provide a guidance on how the short- and medium-range contributions of the NN interaction, as determined by more realistic phase shifts, affect the description of NA scattering in the intermediate energy region. Furthermore, given that the resulting inversion potential is constrained to NN data up to 1.3 GeV in the laboratory frame, meaningful NA scattering studies become feasible at projectile energies as high as $\sim$600 MeV, about twice the limit allowed by the Paris potential.

We have calculated NN inversion potentials from the SM94 data for all NN channels with $L\leqslant 3$. In Fig. 5 we present the phase shifts as a function of the energy for some selected channels. Dots correspond to the SM94 data (only the real part of the phase shifts) and solid curves are the phase shifts from the corresponding SM94 inversion potentials. We also plot the phase shifts obtained from the Paris inversion potentials as reference (dashed curves). These results suggest two observations. One is related to the ability of

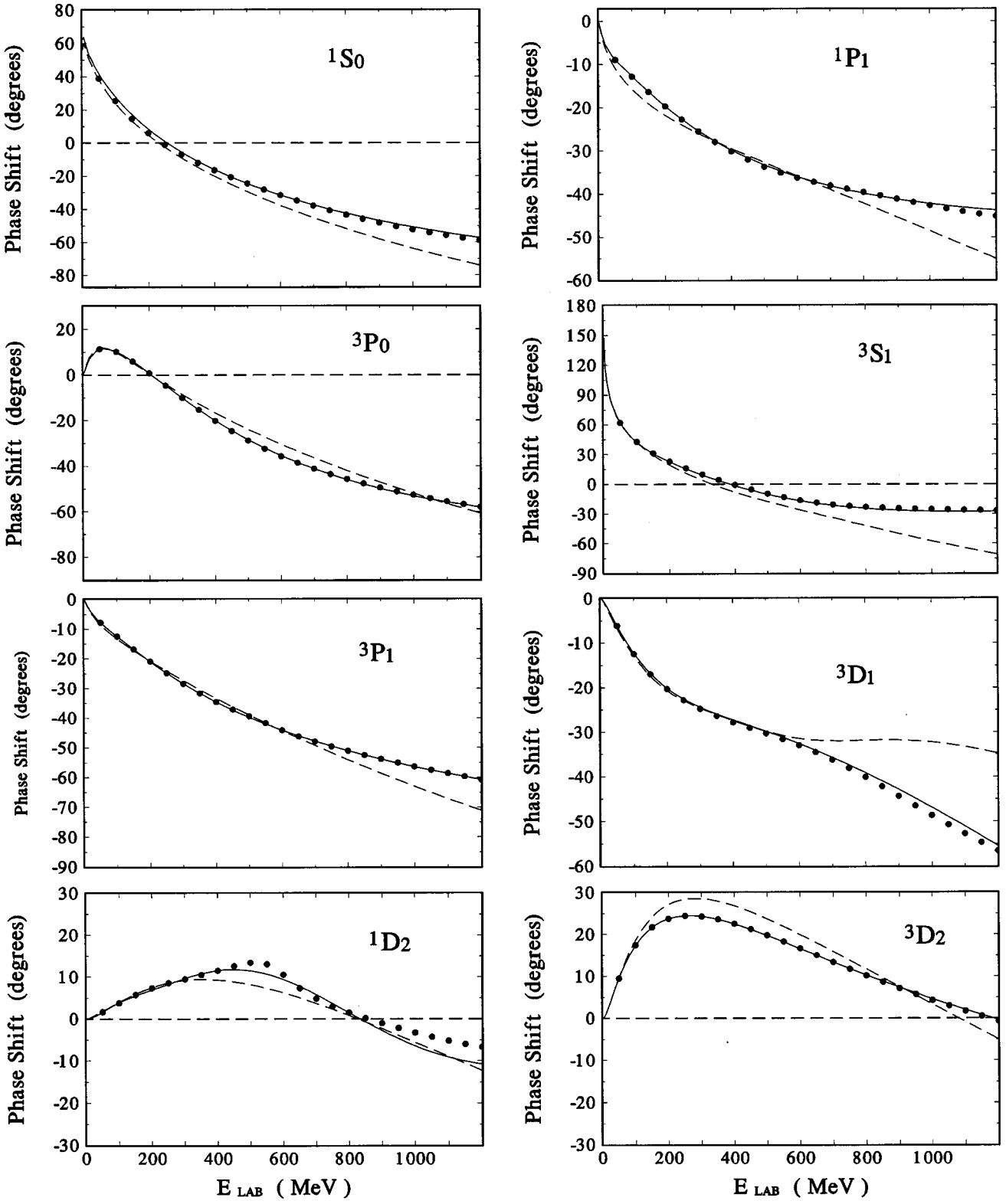

FIG. 5. $L \leqslant 2$ channel real phase shifts from SM94 data (dots), and from the inversion potentials constructed from the real part of the SM94 data (solid curves) and the Paris potential (dashed curves).

the inversion method to reproduce the input data. The accuracy obtained is again excellent and comparable to the Paris case discussed in Sec. III. The other point of physical significance is the clear departure of the Paris phase shifts from, at least, the real part of the experimental ones above pion production threshold. It is precisely the presence of these differences which should affect the overall behavior of the inversion potential and, in particular, its off-shell components.

The calculated *NN* inversion potentials based on the SM94 data have been tested in *NA* elastic scattering. We have performed *in-medium* (g matrix) full-folding calcula-

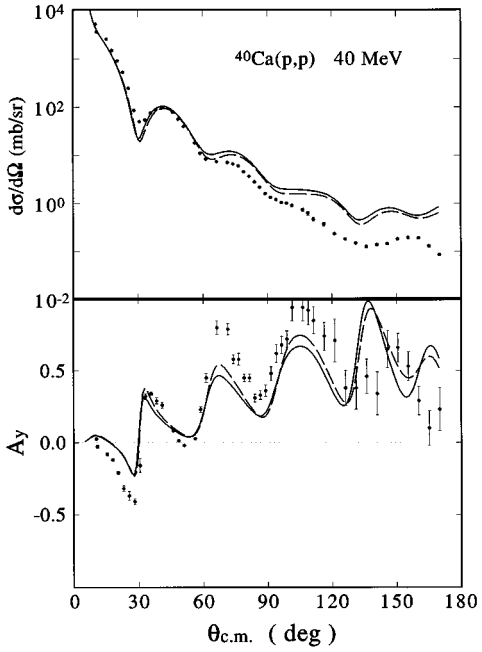

FIG. 6. Calculated and measured differential cross section and analyzing power for $p+{}^{40}$Ca elastic scattering at 40 MeV. The solid and dashed curves were obtained from full folding using the SM94 and Paris inversions, respectively. All curves represent *in-medium* full-folding calculations.

tions for proton scattering from ^{40}Ca at several energies. In these calculations the SM94 inversion potential was used in all NN channels involving $L\leqslant 3$; the genuine Paris potential was used for all the other channels. In Fig. 6 we show the differential cross section and analyzing power for $p+{}^{40}$Ca scattering at 40 MeV. The solid line corresponds to the results from the SM94 inversion potential; the dashed curve represents results from the Paris inversion and they have been included for reference purposes. The differences among the two curves come directly from the fact that the sets of NN phase shifts being used are different. The results shown in Fig. 6 exhibit small differences. This is consistent with the close agreement of both potentials with the NN data below the pion production threshold (see Fig. 5). Since both potentials are constructed following exactly the same inversion procedure, we conclude that phase shifts above 300 MeV still determine properties of the NN potentials which affect low energy NA scattering. These moderate, mostly off shell, differences persist at much smaller energies in many-body systems.

We have pursued scattering calculations at higher energies and other nuclei. In Fig. 7 we present results for $p+{}^{40}$Ca scattering at 200 and 300 MeV. The meaning of the curves is the same as in Fig. 6; the data at 200 and 300 MeV were taken from Ref. [31] and Ref. [32], respectively. At these energies we note a departure among the predictions of the two inversion potentials, with a tendency of the potential based on the NN phase shift data to be closer to the NA scattering data. This result reflects the disagreement between the data and the Paris potential phase shifts (Fig. 5). These findings were confirmed with calculations for $p+{}^{40}$Ca scattering at 400 and 500 MeV. The corresponding results are

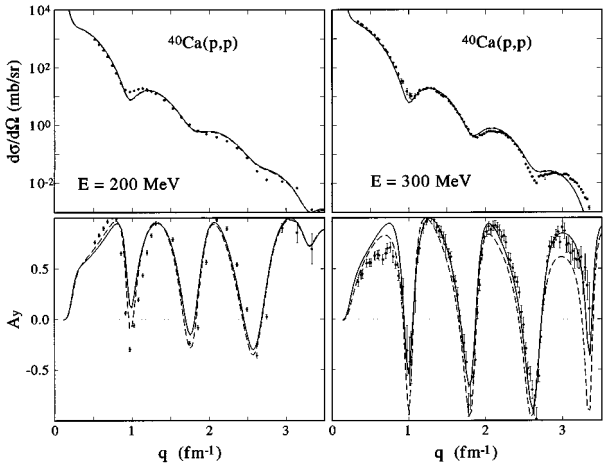

FIG. 7. Calculated and measured differential cross section and analyzing power for $p+{}^{40}$Pb elastic scattering at 200 and 300 MeV. The curve patterns follow convention of Fig. 6.

shown in Fig. 8, where the data at 400 and 500 MeV were taken from Ref. [33] and from Ref. [29] respectively. Certainly, applications of the Paris potential (or its inverse) at 400 MeV and above the constitute an extrapolation of the model. Nevertheless, these applications serve us to illustrate both the role of the NN phase shifts above pion production threshold in determining the NN potential and the ability of the inversion method to capture that physics. The differences given by the two potentials in Fig. 8 are remarkable. In particular, the improvement is notable, obtained in describing the NA scattering observables with the inversion potential constructed from the SM94 data, mainly for $q>1$ fm^{-1} in both $d\sigma/d\Omega$ and A_y. Furthermore, uncertainties associated with the off shell behavior of the NN potential are smaller than the departure of the inversion potentials from the Paris to the SM94 data. This indicates that the improvement in the description of the NA data is a direct consequence of an improved account for the NNdata, mainly above the pion production threshold, a built-in feature in the inversion potential.

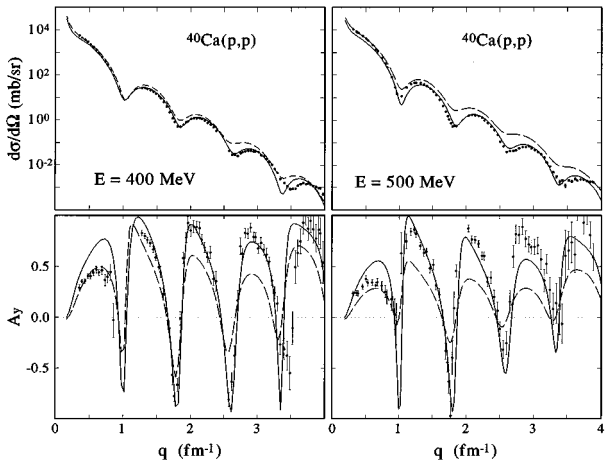

FIG. 8. Calculated and measured differential cross section and analyzing power for $p+{}^{40}$Ca elastic scattering at 400 and 500 MeV. The curve patterns follow convention of Fig. 6.

V. SUMMARY AND CONCLUSIONS

In this paper we have addressed the problem of how properties of the underlying *NN* bare interaction determine the dynamics of a many-nucleon system. Our approach for the *NN* force is based on the quantum inversion method where a local, static, and channel-dependent potential is constructed directly from *NN* phase shifts. By departing from *NN* potentials derived from a field theoretical approach and empirically modified to maximize the fit to *NN* data below the pion production threshold, we expect to shed new light on these properties of the *NN* force relevant to many-body processes.

We have investigated effects associated with the genuine off-shell behavior of bare *NN* potentials which are equivalent from the point of view of the phase shifts over a wide energy range. The construction of on-shell-equivalent potentials was based on the Gelfand-Levitan and Marchenko inversion method for the *NN* system. Applications were made with the Paris potential, where the inversion method was applied to its corresponding phase shifts up to 1.3 GeV kinetic energy in the *NN* laboratory system. This fairly wide energy range was required in order to have the off-shell behavior of the inversion potential determined mainly by the theory and not by the choice of a particular set of phase shifts. The corresponding *NN* effective interactions were found to exhibit sizable differences off-shell, particularly for relative momenta above 3 fm^{-1} in the *NN* system. The investigation of these differences was made in the context of *NA* elastic scattering with the calculation of *in-medium* full-folding optical potentials for proton scattering from ^{40}Ca and ^{208}Pb and at beam energies between 40 and 400 MeV. We found a moderate sensitivity of the *NA* scattering observables to the off–shell differences observed between the *NN* effective interactions. Indeed, differences of at most 10% in the *NA* scattering observables were observed in the whole energy range.

Based on the success of the inversion method to capture the relevant *NN* physics involved in *NA* scattering, we have constructed inversion *NN* potentials based on the SM94 phase shift analysis and used them in full-folding potential calculations. Applications to proton elastic scattering from ^{40}Ca in the 40–500 MeV energy range were made. The results at 40 MeV for the scattering observables yield a fit to the data comparable to that obtained with the Paris potential. However, a departure from the Paris results appears above 200 MeV, with the phenomenological inversion potential providing a superior description of the *NA* scattering data in the 400– and 500–MeV applications. This improvement is a direct consequence of the closer agreement between the inversion potential and the *NN* phenomenology. An important conclusion emerging from this study is that bare *NN* potentials which restrict their fit to *NN* phase shifts below the pion production threshold and disregard their higher energy behavior are unlikely to be realistic candidates to describe the nucleon-nucleon dynamics in the nuclear medium.

Despite the improvements in the description of *NA* scattering using inversion potentials from *NN* data, particularly at the high energies, difficulties do remain in describing the *NA* scattering data at momentum transfers below 1 fm^{-1}. We believe the explicit treatment inelasticities of the *NN* interaction above the pion production threshold and baryon excitation mechanisms need to be addressed as the inversion potentials from the SM94 analysis were restricted to the real part of the phase shifts. On the other hand, in the low energy applications we observe a systematic inability of the full-folding model to describe in certain detail the *NA* scattering data. Here, the presence of higher order processes needs definitely to be accounted for. Indeed, the results obtained at these energies using the Paris potential, its inversion, and the SM94 inversion provide essentially the same description of the *NA* scattering data. Therefore, the limitations of the optical model at these low energies cannot be attributed to uncertainties associated with the off shell behavior of the *NN* interaction.

ACKNOWLEDGMENTS

H.F.A. is grateful for the hospitality of the nuclear theory group of the Theoretische Kernphysik, Universität Hamburg. This research was supported in part by FONDECYT Grants Nos. 3940008 and 1931115, and the Forschungszentrum Jülich COSY Collaboration Grant No. 41126865.

[1] M. K. Srivastava and Donald W. L. Sprung, in *Advances in Nuclear Physics*, edited by Michel Baranger and Erich Vogt, (Plenum Press, New York, 1975), Vol. 8.
[2] M. Lacombe, B. Loiseau, J. M. Richard, R. Vinh Mau, J. Côté, P. Pirés, and R. de Tourreil, Phys. Rev. C **21**, 861 (1980).
[3] R. Machleidt, K. Holinde, and Ch. Elster, Phys. Rep. **149**, 1, (1987).
[4] V. G. J. Stocks, R. A. M. Klomp, C. P. F. Terheggen, and J. J. de Swart, Phys. Rev. C **49**, 2950 (1994).
[5] M. Jetter and H. V. von Geramb, Phys. Rev. C. **49**, 1832 (1994); M. Jetter, H. Kohlhoff, and H. V. von Geramb, in *Quantum Inversion Theory and Applications*, edited by H. V. von Geramb (Springer-Verlag, Berlin, 1994), p. 342.
[6] M. Jetter and H. W. Fearing, Phys. Rev. C **51**, 1666 (1995).
[7] H. F. Arellano, F. A. Brieva, and W. G. Love, Phys. Rev. C **41**, 2188 (1990).
[8] H. F. Arellano, F. A. Brieva, and W. G. Love, Phys. Rev. C **50**, 2480 (1994).
[9] H. F. Arellano, F. A. Brieva, and W. G. Love, Phys. Rev. C **52**, 301 (1995).
[10] Ch. Elster, T. Cheon, E. F. Redish, and P. C. Tandy, Phys. Rev. C **41**, 814 (1990).
[11] R. Crespo, R.C. Johnson, and J.A. Tostevin, Phys. Rev. C **41**, 2257 (1990).
[12] L. Ray, G. W. Hoffmann, and W. R. Coker, Phys. Rep. **212**, 223 (1992).
[13] H. F. Arellano, F. A. Brieva, W. G. Love, and K. Nakayama, Phys. Rev. C **43**, 1875 (1991).
[14] M. M. Nagels, T. A. Rijken, and J. J. de Swart, Phys. Rev. D **12**, 768 (1978).
[15] L. Rikus and H. V. von Geramb, Nucl. Phys. **A426**, 496 (1984).

[16] H. V. von Geramb and H. Kohlhoff, in *Quantum Inversion Theory and Applications*, edited by H. V. von Geramb (Springer-Verlag, Berlin, 1994), p. 285; H. Kohlhoff and H. V. von Geramb, *ibid.*, pp. 314.
[17] Th. Kirst, K. Amos, L. Berge, M. Coz, and H. V. von Geramb, Phys. Rev. C **40**, 912 (1989).
[18] A. L. Fetter and K. M. Watson, in *Advances in Theoretical Physics*, edited by K.A. Brueckner (Academic Press, New York, 1965), Vol. 1.
[19] H. Feshbach, Ann. Phys. (N.Y.) **5**, 357 (1958); **19**, 287 (1962).
[20] A. K. Kerman, H. McManus, and R. M. Thaler, Ann. Phys. (N.Y.) **8**, 551 (1959).
[21] J. M. Eisenberg and D. S. Koltun, *Quantum Many-Particle System* (John Wiley, New York, 1989).
[22] Leo P. Kadanoff and Gordon Baym, *Quantum Statistical Mechanics* (Addison-Wesley, Reading, MA, 1989).
[23] X. Campi and A. Bouyssy, Phys. Lett. **73B**, 263 (1978).
[24] H. F. Arellano, F. A. Brieva, and W. G. Love, Phys. Rev. C **42**, 652 (1990).
[25] J. P. Jeukenne, A. Lejeune, and C. Mahaux, Phys. Rep. C **25**, 83 (1976).
[26] S. K. Adhikari and K. L. Kowalski, *Dynamical Collision Theory and Its Applications* (Academic Press, New York, 1991).
[27] R. H. McCamis *et al.*, Phys. Rev. C **33**, 1624 (1986).
[28] L. N. Blumberg, E. E. Gross, A. van der Woude, A. Zucker, and R. H. Bassel, Phys. Rev. **147**, 812 (1966).
[29] D.A. Hutcheon *et al.*, Nucl. Phys. **A483**, 429 (1988).
[30] R. A. Arndt, I. I. Strakovsky, and R. L. Workman, Phys. Rev. C **50**, 2731 (1994).
[31] J. J. Kelly *et al.*, Phys. Rev. C **39**, 1222 (1989).
[32] E. J. Stephenson, J. Phys. Soc. Jpn. (Suppl.) **55**, 316 (1985).
[33] E. Bleszynski *et al.*, Phys. Rev. C **37**, 1527 (1988).